Supplementary Methods

Analysis of time course gene expression data. The time course data of the expression level of a representative gene is shown in the below figure. The trajectory of longitudinal expression of each gene was obtained by a cubic spline function, and the mean expression of controls was considered as the base line expression. The maximum deviation of the trajectory line from the base line was referred to as the maximum fold change, or simply the fold change of the gene between patients and healthy controls. For each gene, the time required for the gene to change to the half of its maximum fold change was defined as its response time, and the time required for the gene to return back to the half after reached maximum point was defined as its recovery time. The significance of the longitudinal gene expression change was estimated using EDGE (1) by 1,000 random permutations. Significant genes were selected by FDR<0.001 and fold change ≥2 for each data sets. 5,544 genes were identified as significant between patients and healthy subjects (4,389 in trauma, 3,250 in burns, and 2,251 in endotoxemia).

Analysis of the longitudinal gene expression. Shown is the time course data of the measured expression level of a representative gene. On the x-axis, points of samples of controls are displayed at 0 hour, and points of patient samples are displayed according to their sampling time after injury. On the y-axis, each point shows the log2 fold change of the expression value of the gene in one sample compared with the mean expression of the controls. The longitudinal trend line (in green) was obtained by spline smoothing of the gene expression values. The maximum fold change is defined as the largest deviation of the trend line from the base level, i.e. the mean expression of the controls. The response time and recovery time are defined as the time when the trajectory reaches half of the maximum fold change before and after reaching the maximum respectively.

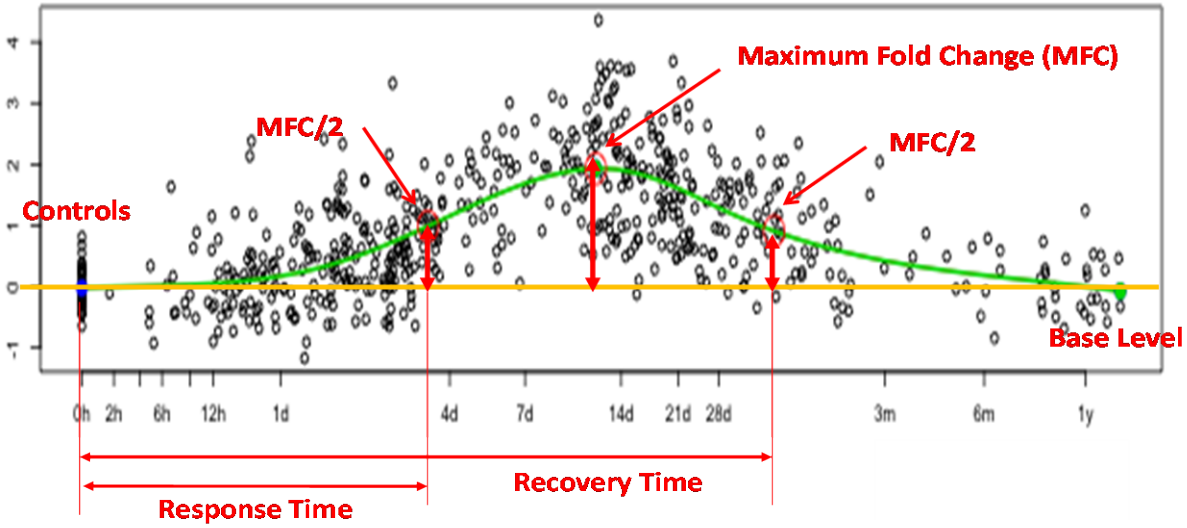

Human-mouse orthologs. 20,273 Entrez genes were assayed on Affymetrix human HU133 plus v2 arrays, among which 16,646 had mouse orthologs according to the Mouse Genome Database (2), and 15,686 were assayed on Affymetrix mouse MOE430 arrays. Among the 5,554 genes significantly changed in human conditions, 4,918 genes had mouse orthologs assayed on the mouse arrays, which were included in the subsequent analysis.

Comparison of gene response between datasets. The maximum fold changes of gene expression were measured in log-scale between patients and healthy subjects for each data set of human burn, trauma and endotoxemia, and between treated group and control group for the corresponding murine models. Between two datasets, the agreements of the maximum gene fold changes (R^2) as well as directionality of the changes (%) were compared. R^2 represents the square of Pearson's correlation. Similar results were seen when the rank correlation was calculated as in Fig. S1. % represents the percentages of genes changed to the same direction between the two datasets.

In Fig. S9, gene expression changes of patients subjected to irradiation were compared with those of mouse models (GSE10640) (3, 4). Gene expression data was obtained from GSE10640, which includes two independent sets of patients under irradiation as part of their pre-transplantation conditioning (n=24 and 10, each set was assayed on a different microarray platform) and 11 mouse models. 487 significantly changed genes (FDR<0.05) between patients under irradiation and controls were identified. R^2 and % were calculated in these genes between the first data set of patients (n=24) and the second set of patients (n=10) and the mouse models.

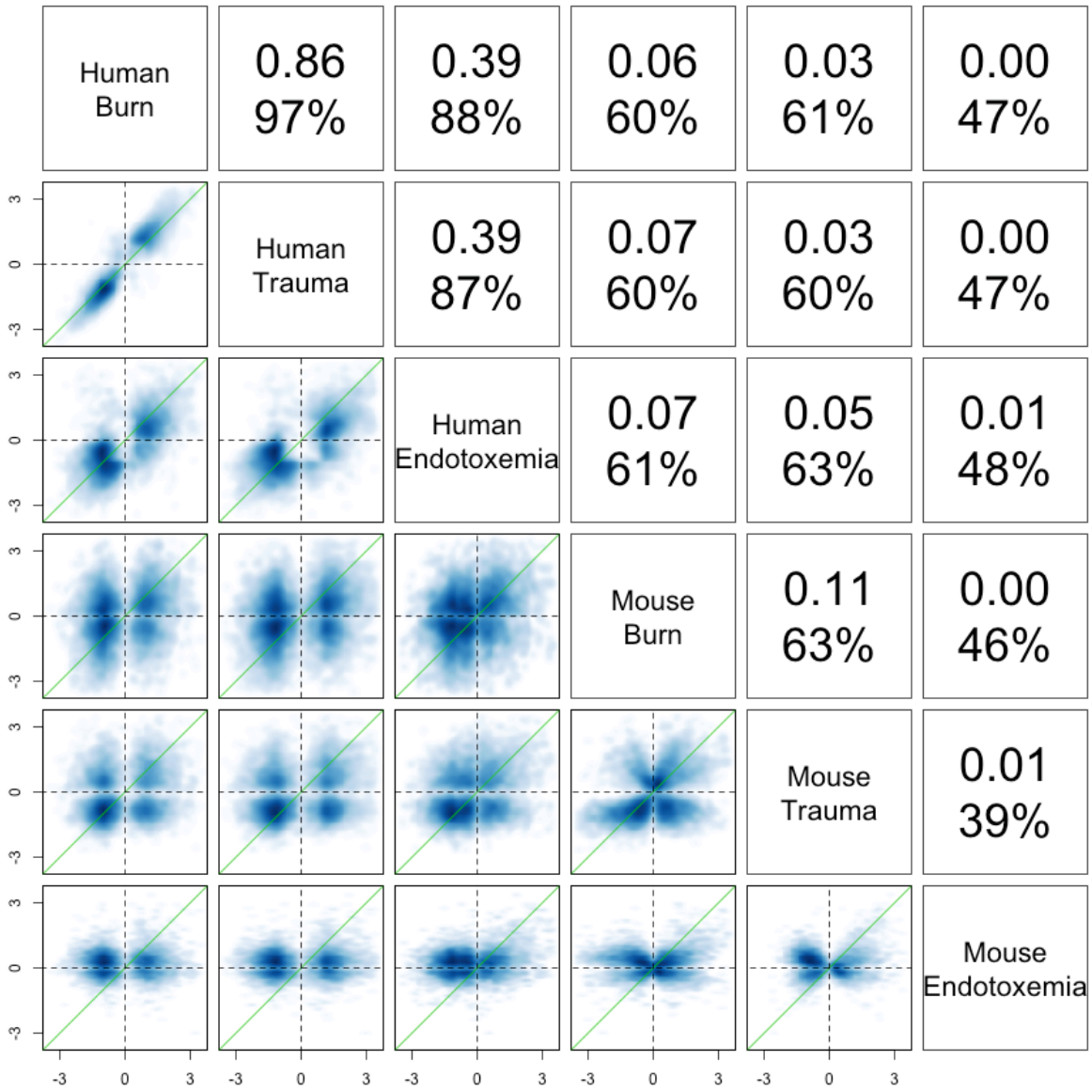

Fig. S1. Rank correlations (R^2) and percentages of genes changed to the same direction (%) between the human and mouse studies. The lower left half of the figure shows the scatter plots of the log2 fold changes of 4,918 human genes responsive to trauma, burns or endotoxemia (FDR<0.001; fold change >2), the same as shown in Fig. 1. The upper right half lists the rank correlations (R^2) and percentages of genes changed to the same direction (%) between the corresponding studies. Note that by random chance 50% of the genes between two uncorrelated conditions are expected to change in the same direction. The results show that the genomic responses to human trauma and burns are highly correlated, while the murine models correlate poorly with human conditions and each other.

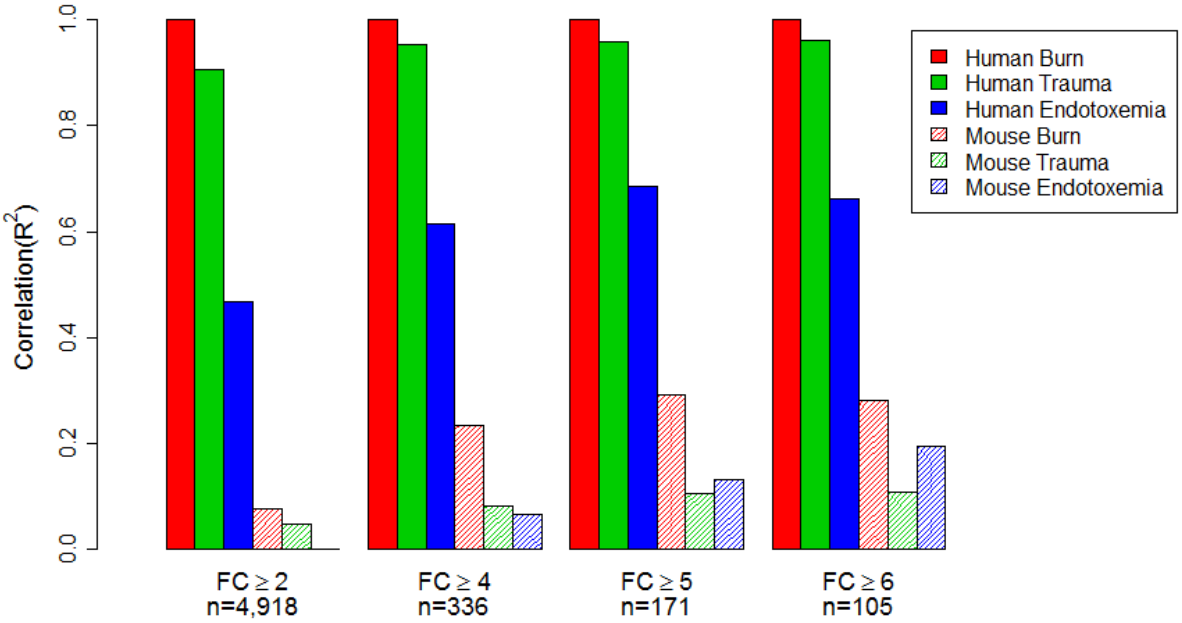

Fig. S2. Correlations of gene changes between the human and murine studies in subsets of genes significantly changed in human injury and showed a greater magnitude of fold changes (FC). Among 4,918 human genes significantly changed in human trauma, burns or endotoxemia (FDR<0.001; FC≥2), 336 genes had FC≥4, 171 had FC≥5, and 105 had FC≥6 in human burn. Shown are bar graphs of Pearson correlations (R^2) between human trauma, endotoxemia, three murine models versus human burns as a reference. While the murine models correlate poorly among the 4,918 genes significantly changed in human injuries (FDR<0.001; FC≥2) with the corresponding human conditions (R^2=0.00-0.09), the correlations increase to (R^2=0.11-0.28) among the top 105 genes with the greatest magnitude of changes (FDR<0.001; FC≥6).

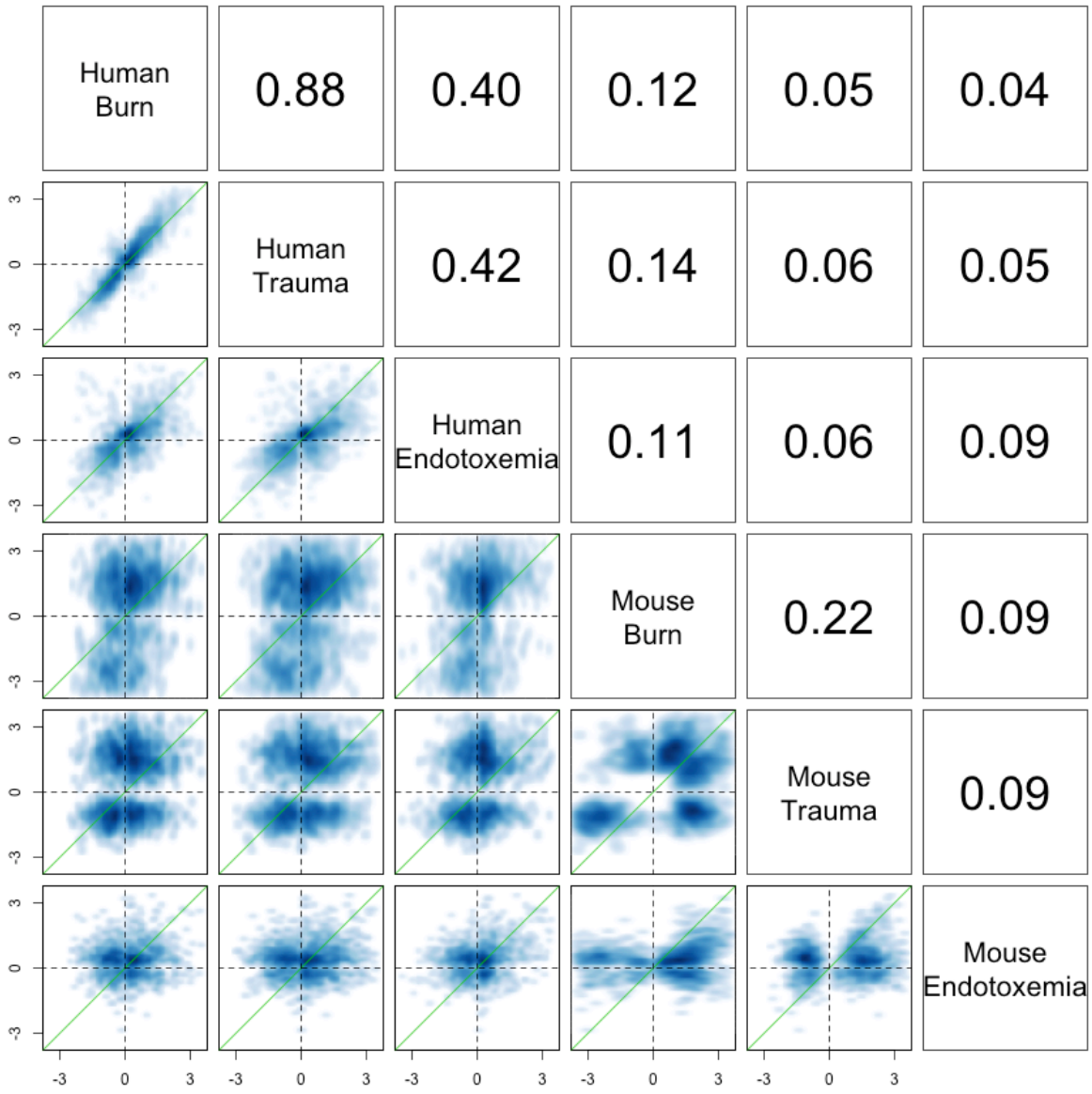

Fig. S3. Scatter plots and Pearson correlations (R^2) of genes significantly changed in the murine models. In the mouse models, 1,519 genes were significant at FDR<0.001 and ≥2 fold changes between the treated and control groups in either one of the three murine models, among which 87% (1,318) have human orthologs. In contrast to the 4,918 genes responsive to one of the human conditions as shown in Fig. 1, here the scatter plots depict fold changes of these 1,318 genes. The axes represent log2 fold changes. The high correlation was maintained in these genes between human trauma and burn (R^2=0.88), whereas correlation between models was low (R^2≤0.22).

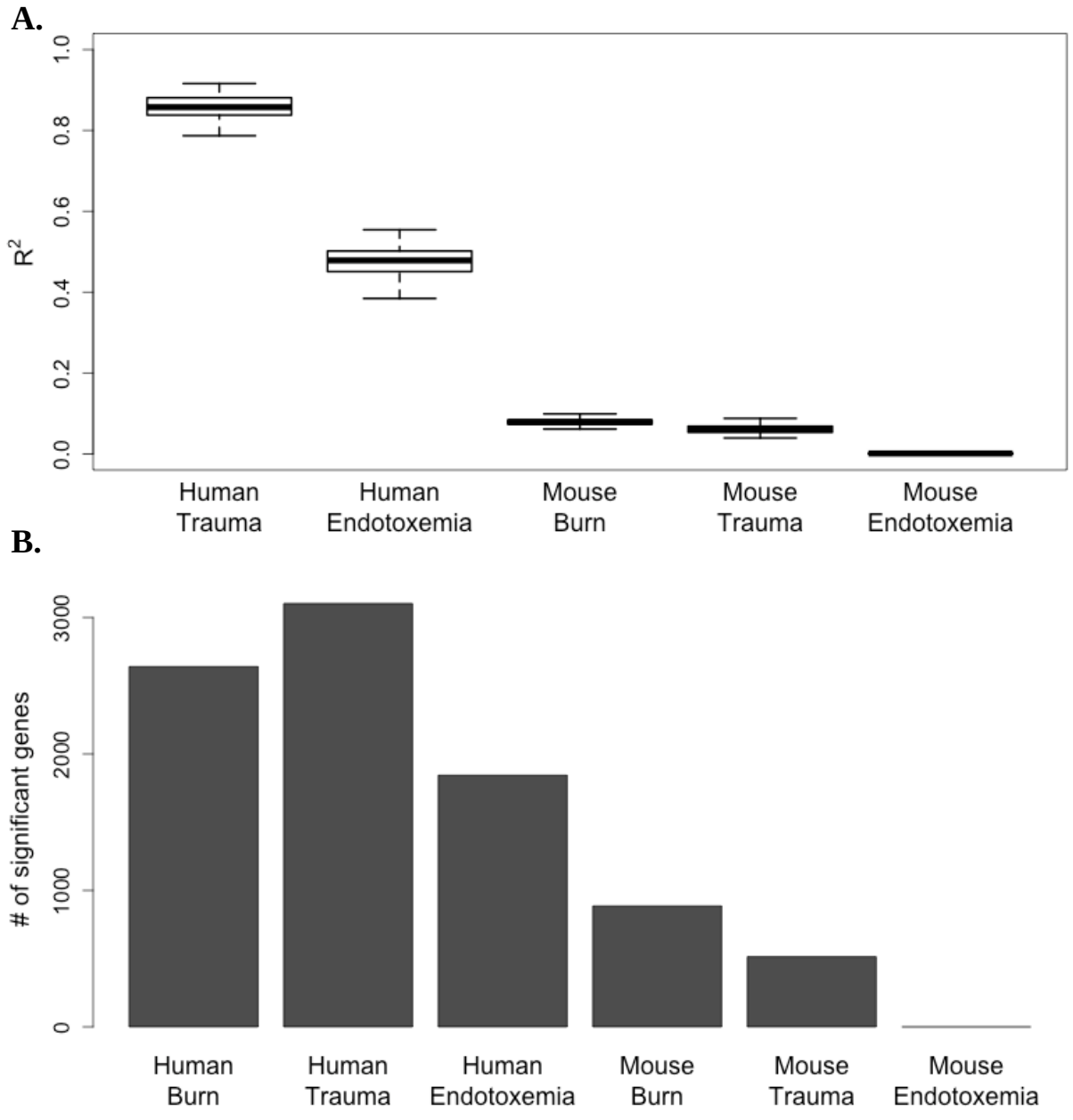

Fig. S4. Robustness of the analysis with respect to the sample sizes. The two human injury studies included 167 trauma patients sampled over the first 28 days after injury, 244 burn patients over the first year after injury, and 37 healthy controls, while the human endotoxemia study included 4 healthy volunteers received bacterial endotoxin and 4 controls each measured at four time points. The mouse models of trauma, burns, and endotoxemia each included 16 mice as the treated group and 16 as the control group (four time points, and 4 treated and 4 controls at each time point). To address the potential confounding feature of different sample sizes between the studies, comparable numbers of humans and mice were compared by random resampling. Since significant genes in the mouse burn and trauma models were identified from the time

course changes over four time points after injury, to simulate a similar environment in the human injury studies, we randomly selected four burn subjects at 3 days (0-3d), 7 days (3d-7d), 14 days (7d-14d), and 21 days (14d-21d) as well as four healthy controls at each time point, and then measured the significance of each gene with the same method applied to the mouse data. For human trauma, four trauma subjects were randomly selected at 1 day (0-1d), 4 days (2d-4d), 7 days (4d-7d), and 14 days (7d-14d) as well as the controls. The comparison was repeated by 1,000 times. **(A)** Box plots of the correlations (R^2) between burn injury and the other human conditions and murine models. The maximum fold changes of the randomly selected burn patients were compared with those of randomly selected trauma patients as well as the maximum fold changes from human endotoxemia and murine models. The correlations remained high between human injuries (R^2 =0.85). **(B)** The number of significantly changed genes detected in each human condition and murine model. For the human injuries, the time course of the randomly selected burn and trauma patients and controls were analyzed and the number of significant genes were identified (FDR<0.001 & FC≥2). The median of the results from the 1,000 repeats is shown for human burns and trauma. Human conditions cause much more profound genomic response (≥ 3x more genes) than the corresponding mouse models.

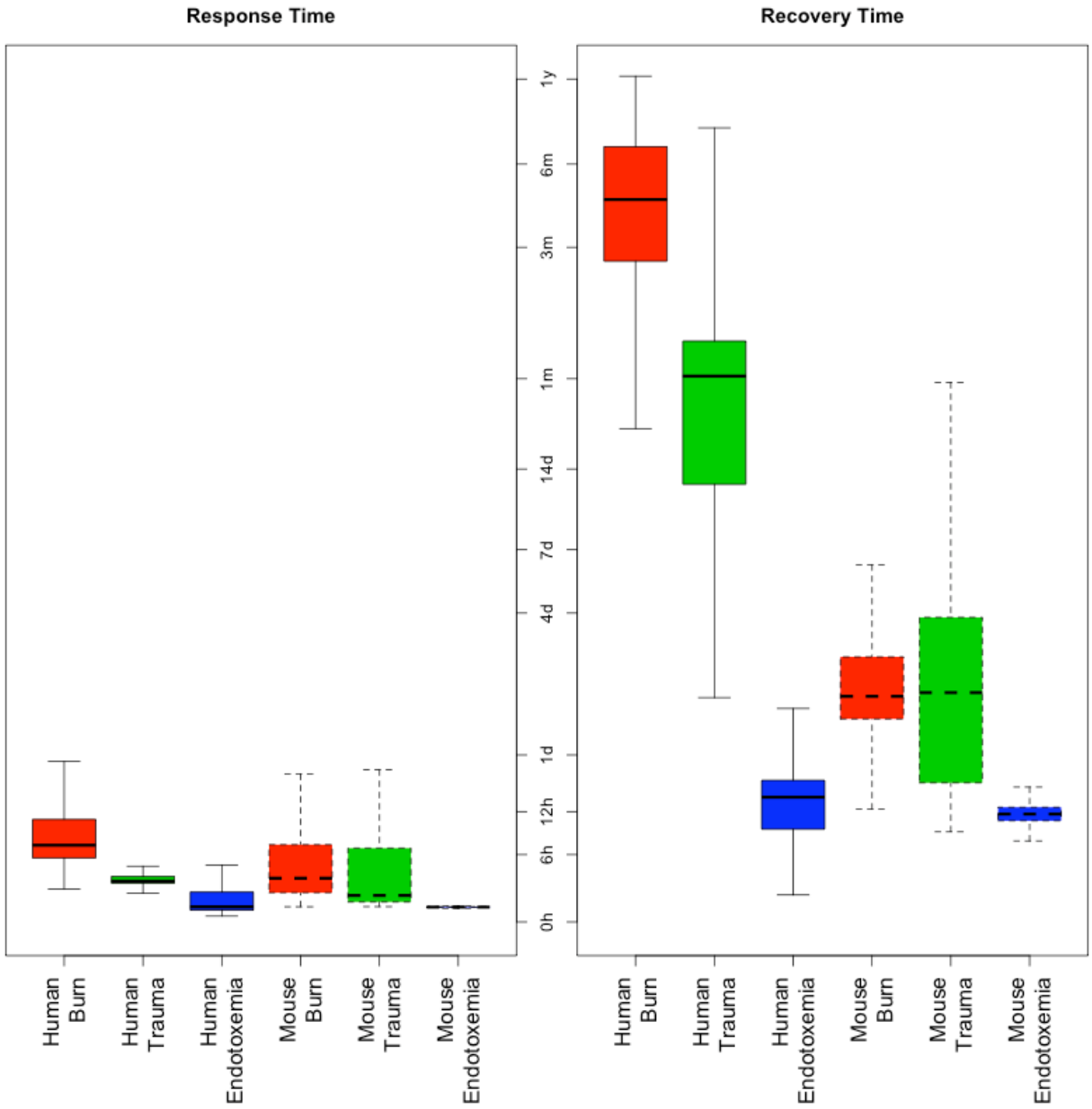

Fig. S5. Box plots of the response and recovery times of gene expression in human burns, trauma and endotoxemia as well as corresponding mouse models. The response time is the time when the gene fold change reaches half of the maximum change. The recovery time is the time when the gene fold change returns back to half after it reached the maximum. While most of the gene response (75% percentile) occurred within the first 12 hours in all of the human injuries (human burns and trauma) and models (human endotoxemia and the three mouse models), the recovery differed dramatically in the time scale. The genomic disturbance in the models recovered within hours to 4 days (75% percentile), but lasted for 1-6 months in trauma and burn patients.

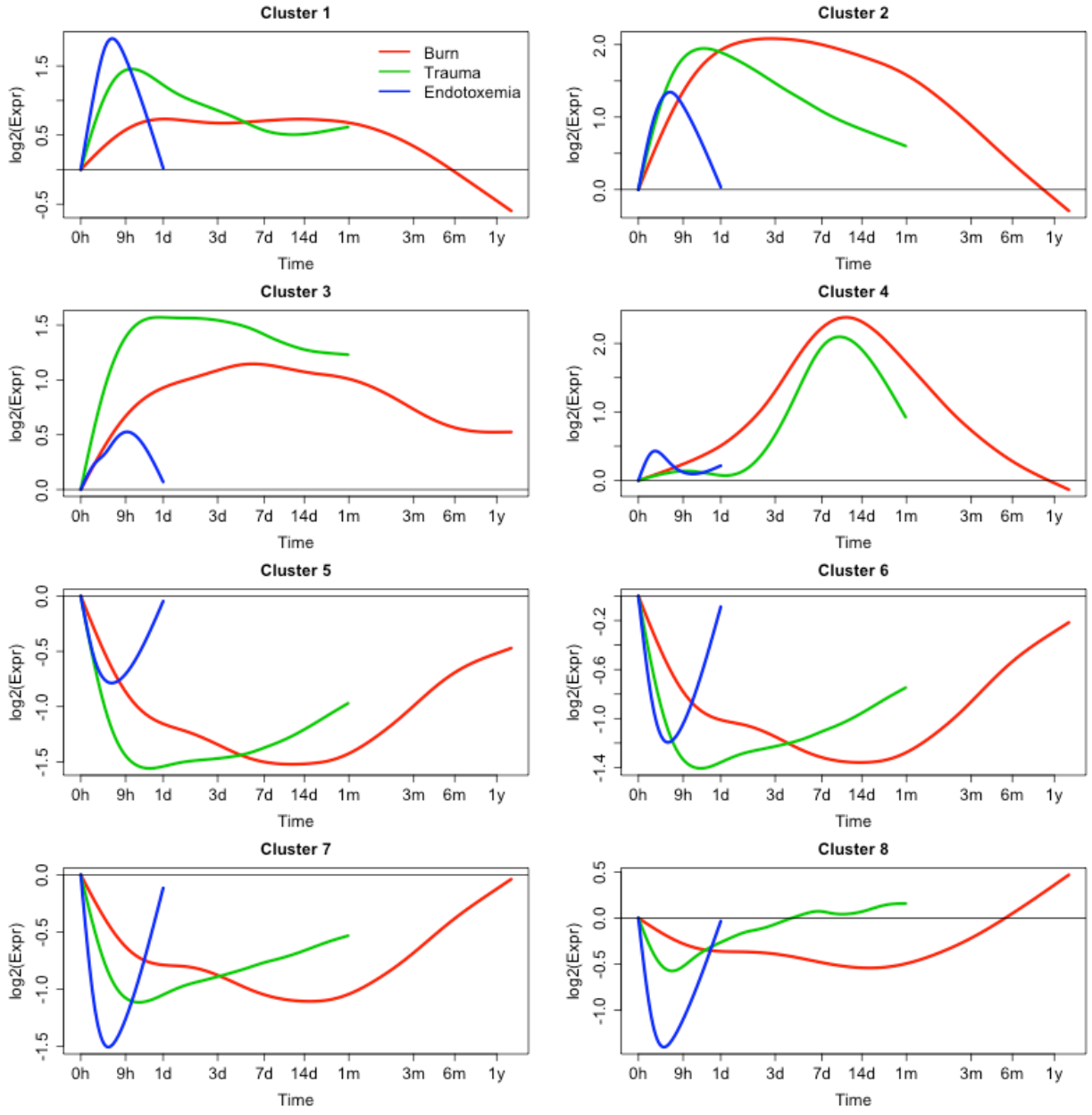

Fig. S6. Centroid expression of each gene cluster in human as shown in Fig. 2A. Each panel describes the centroid expression of a gene cluster for the three human conditions. The longitudinal trend lines were obtained by spline smoothing. Clusters 1-3 depict the common early activation (35% of the genes in Fig. 2A), clusters 5-8 are for the common early suppression (60%), and cluster 4 presents the late activation specific to burn and trauma (5%). Most of the genes changed in the same direction between burns and trauma (97%) and between the two injuries and endotoxemia (88%). In addition, the gene response time was within hours to burns, trauma and endotoxemia, while gene recovery differed dramatically between hours for endotoxemia, one month for trauma, and six months for burns.

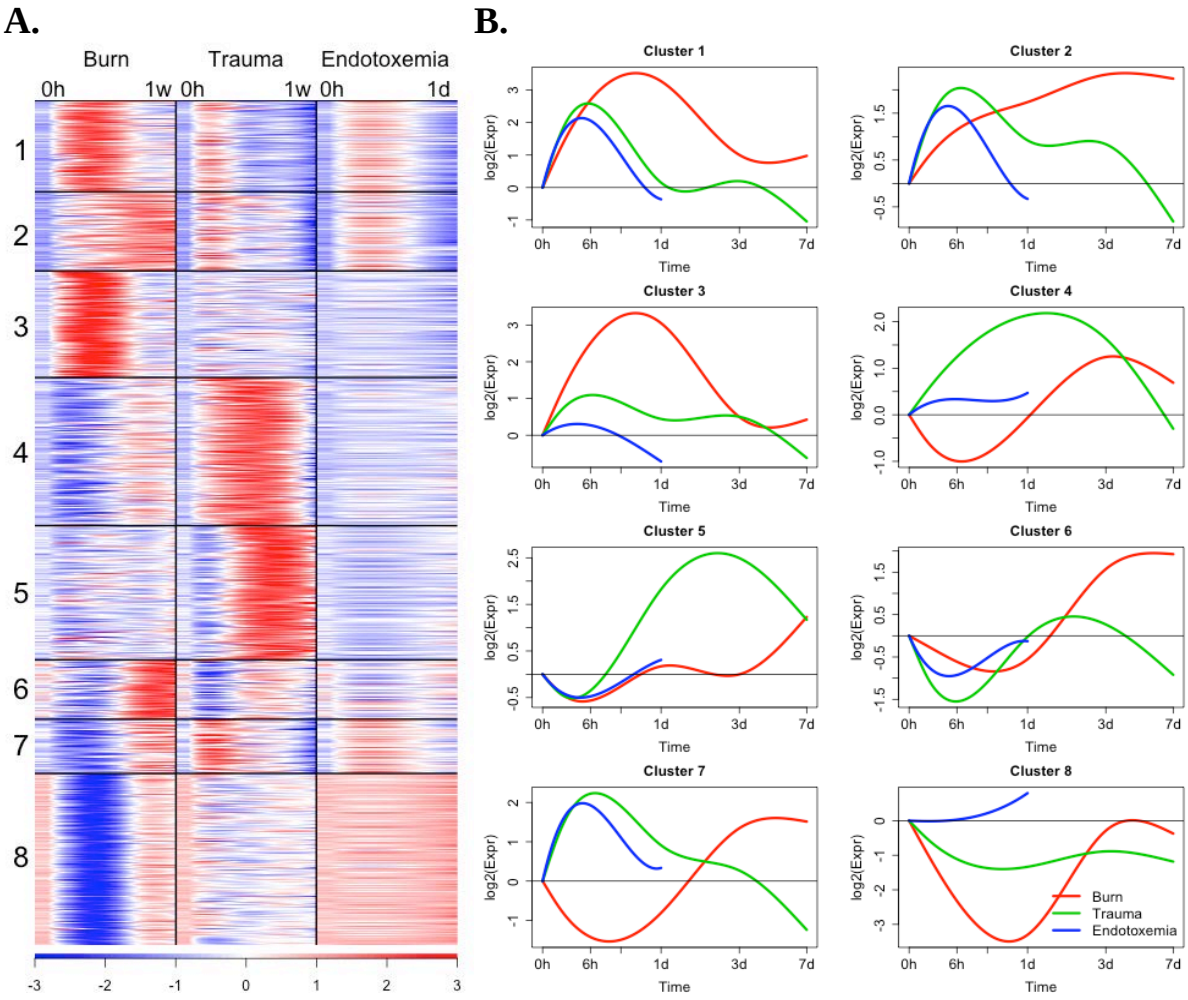

Fig. S7. Gene changes over time for the genes responsive in the murine models. 1,519 genes were differentially expressed between the treated and control groups (FDR< 0.001 and ≥2-fold change). **(A)** K-means clustering of genes over time. Red indicates increased and blue indicates decreased expression relative to the mean (white). **(B)** Centroid expression of each gene cluster in the murine models. Each panel describes the centroid expression of a gene cluster for the three murine models. The longitudinal trend lines were obtained by spline smoothing. There was great variability among the three murine models within each cluster for the time span, suggesting that mouse gene responses differed from one another.

A. Toll-like receptor expression in human burns

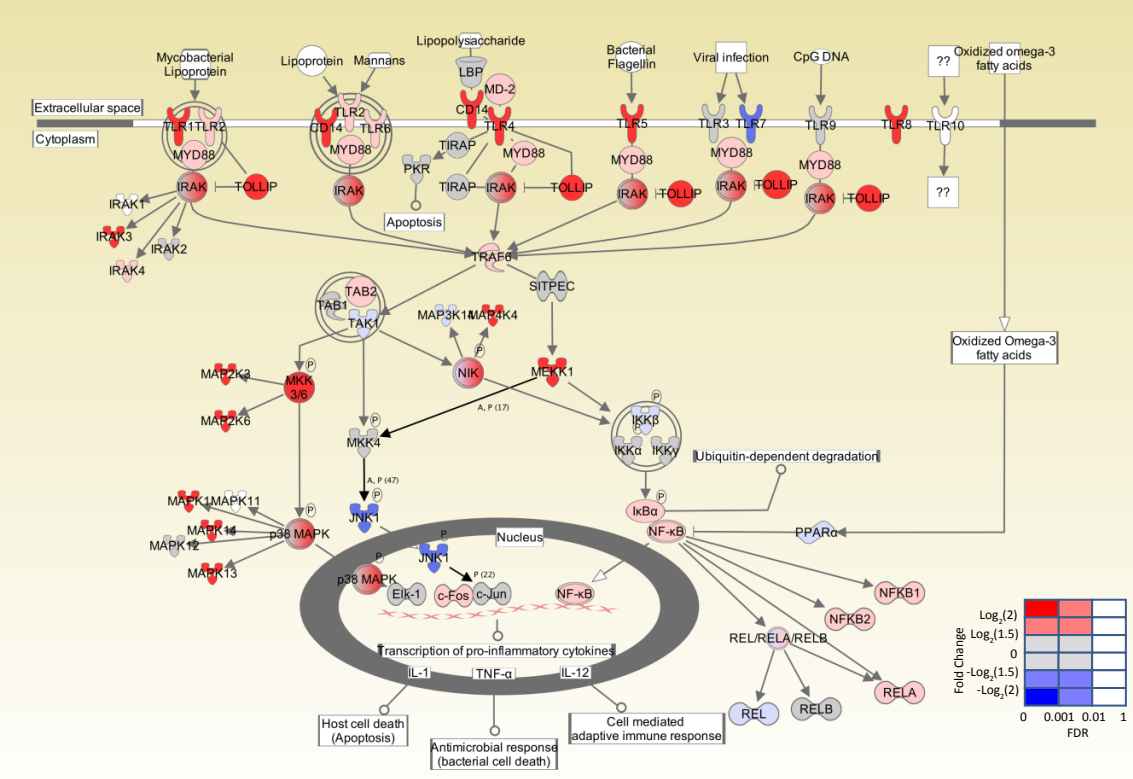

B. Toll-like receptor expression in the murine burns model

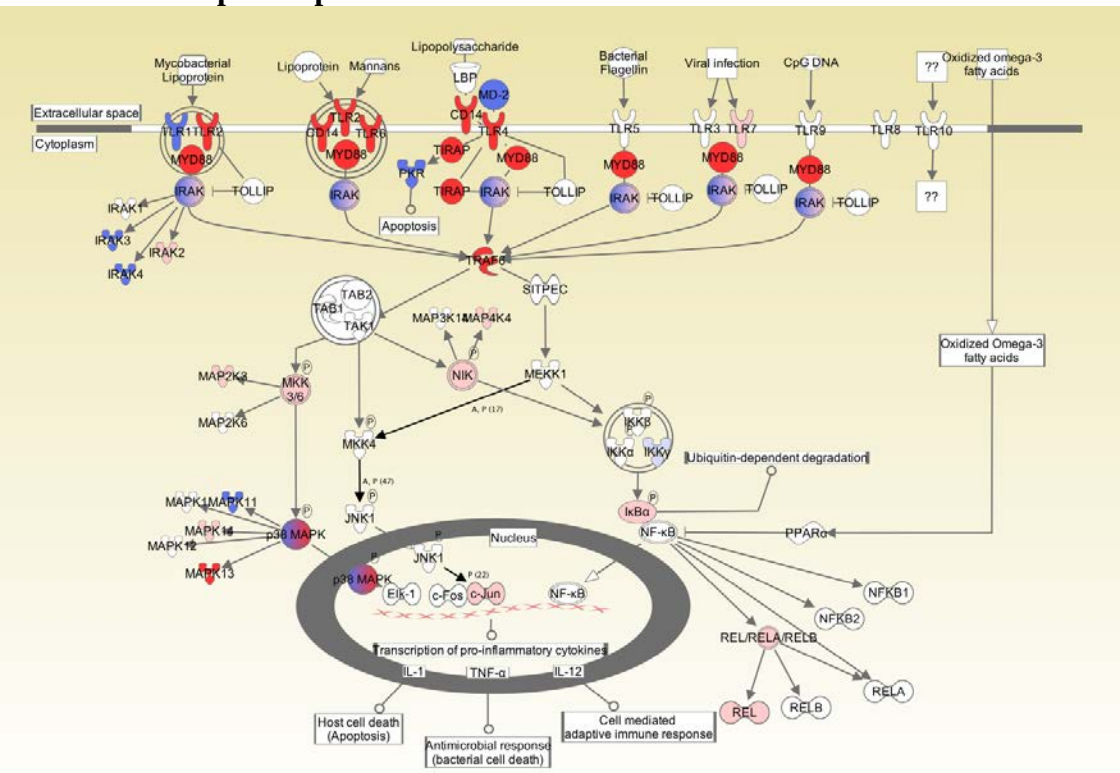

C. Toll-like receptor expression in human trauma

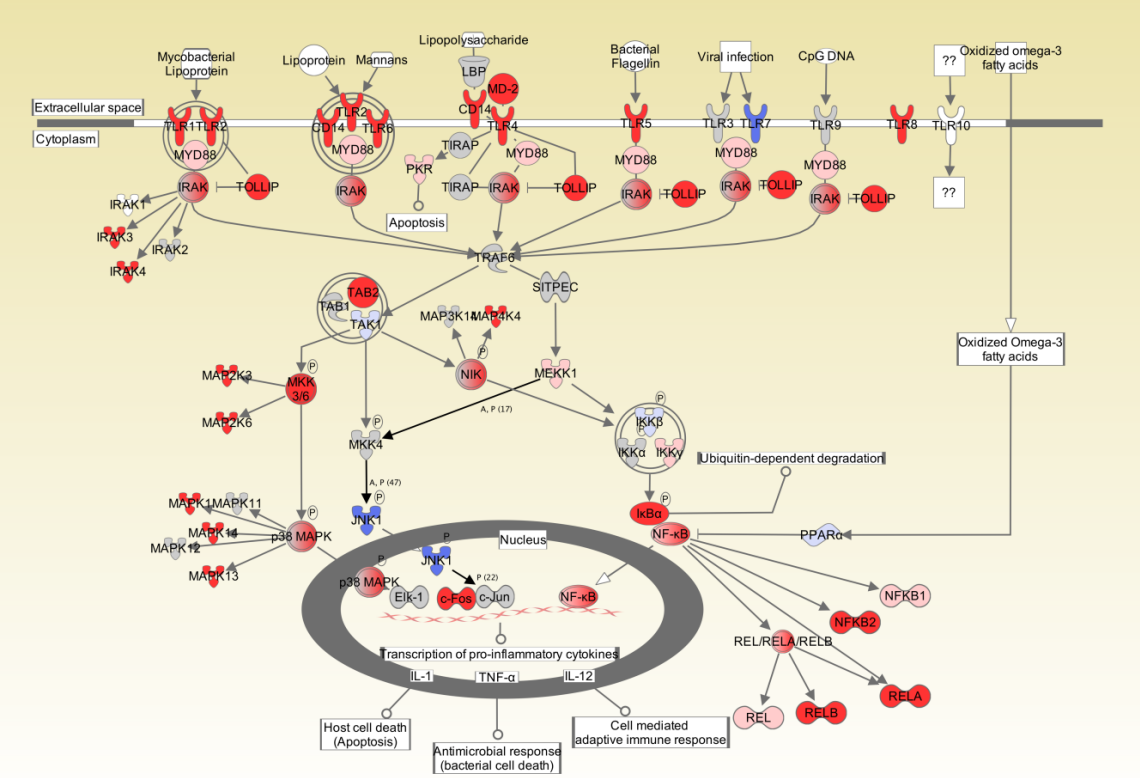

D. Toll-like receptor expression in the murine trauma model

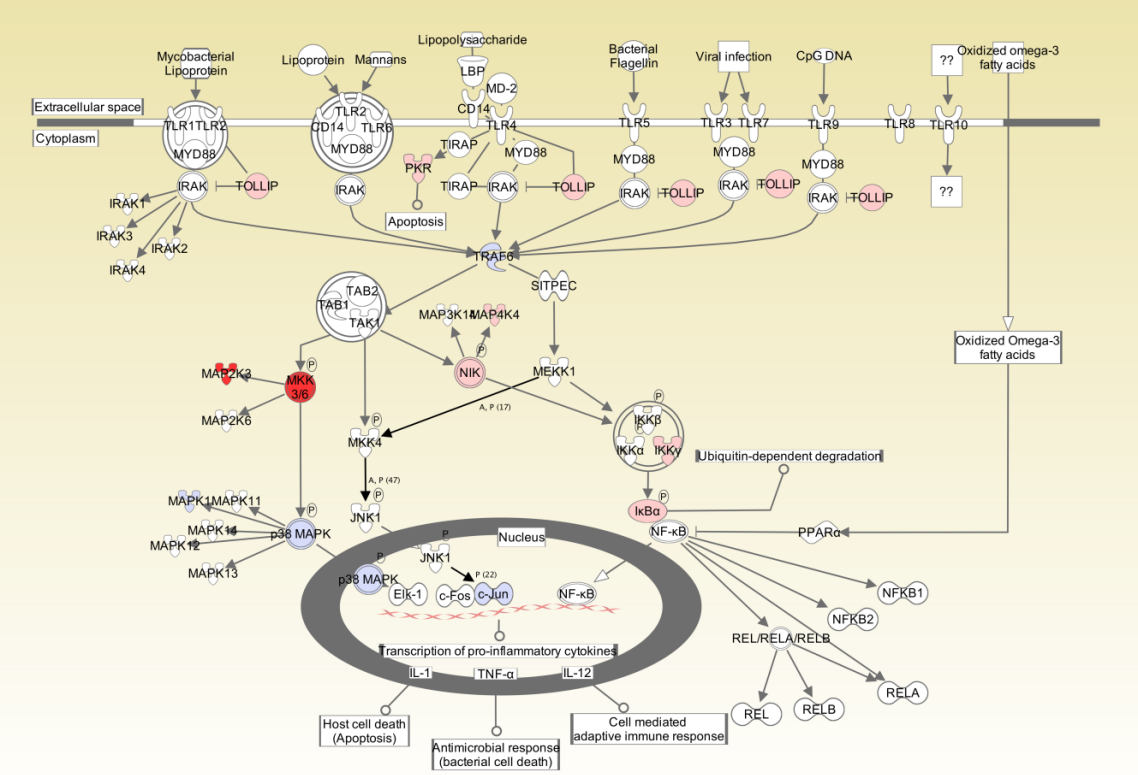

E. Toll-like receptor expression in human endotoxemia

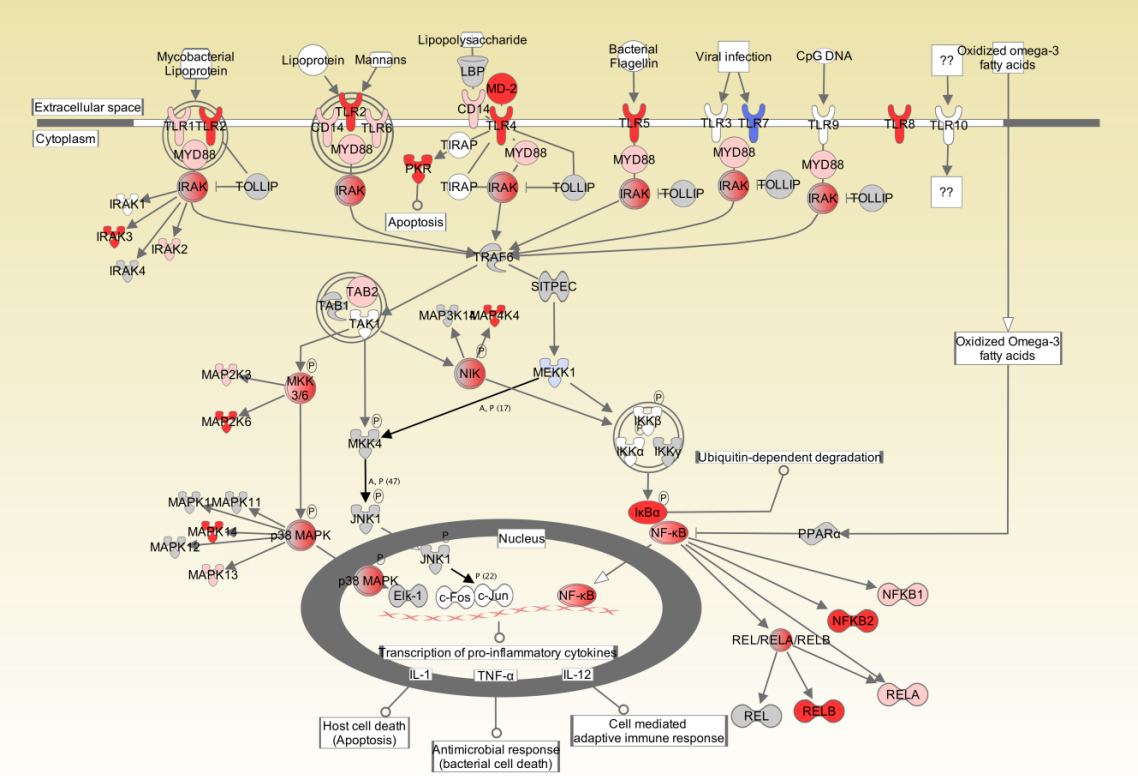

F. Toll-like receptor expression in the murine endotoxemia model

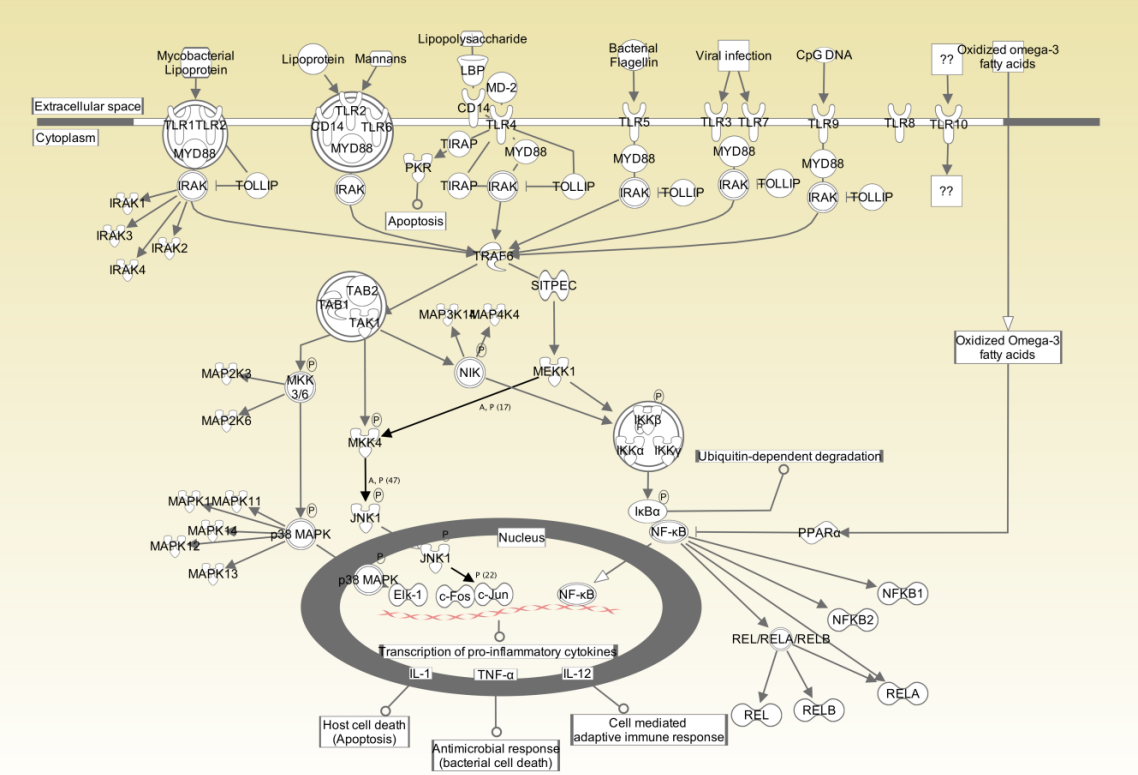

Fig. S8. The changes of genes in the TLR pathways for human injuries and the mouse models. Genes with FDR<0.01 are colored, and the rest genes are in white. Genes with significant changes (FDR<0.001 and fold change ≥2) are colored in red if activated or blue if suppressed. Genes with mild changes (FDR<0.01 and fold change ≥1.5) are colored in light red or light blue. Other genes (FDR<0.01 but fold change<1.5) are colored in gray. Toll-like receptor expression in **(A)** human burns, **(B)** the murine burns model, **(C)** human trauma, **(D)** the murine trauma model, **(E)** human endotoxemia, and **(F)** the murine endotoxemia model.

Fig. S9. Comparison of gene expression changes by radiation exposure in mice and patients. Gene expression data was obtained from GSE10640 (3, 4), which includes two independent sets of patients under irradiation as part of their pre-transplantation conditioning (n=24 and 10) and 11 mouse models. 487 significantly changed genes (FDR<0.05) between patients under irradiation and controls were identified. Plotted are the correlations (R^2, left, pink) of the fold changes of these genes and the percentages of genes changed in the same direction (%, right, green) between the first data set of patients (n=24) and the second set of patients (n=10) and the mouse models.

Table S1. Reproducibility of human and mouse studies. Standard deviations (SD) and coefficients of variation (CoV) were calculated from the biological replicates at each time point and averaged over the time points for mouse experiments and human endotoxemia. For human trauma and burn patients, the SD and CoV were calculated from samples of each binned time as described in **Fig. S4** and averaged over the bins.

Table S1.		
	SD	CoV
Human Controls	0.2986	0.053
Human Burn	0.3606	0.060
Human Trauma	0.2474	0.042
Human Endotoxemia	0.1456	0.061
Mouse Controls	0.2389	0.058
Mouse Burn Model	0.2378	0.058
Mouse Trauma-Hemorrhage Model	0.3204	0.078
Mouse Endotoxemia Model	0.2090	0.051

Table S2. Pathway comparisons between human injuries and mouse models. Shown are Pearson correlations (R^2) and percentages of genes changed to the same direction (%) for **(A)** the 20 most up-regulated and **(B)** the 20 most down-regulated pathways between the four model systems (human endotoxemia and the three murine models) versus human burn injury. Negative correlations are shown as negative numbers ($-R^2$). Human trauma is shown as reference. In every pathway, human endotoxemia had much higher similarity to human injury than mouse models had.

Table S2A	# Genes	Human Trauma (R^2)	Human Trauma (%)	Human Endotoxemia (R^2)	Human Endotoxemia (%)	Mouse Burn (R^2)	Mouse Burn (%)	Mouse Trauma (R^2)	Mouse Trauma (%)	Mouse Endotoxemia (R^2)	Mouse Endotoxemia (%)
Fcγ Receptor-mediated Phagocytosis in Macrophages and Monocytes	46	0.96	100%	0.63	93%	0.04	63%	-0.04	37%	0.16	72%
IL-10 Signaling	33	0.95	100%	0.68	91%	0.49	79%	0.22	67%	0.43	79%
Integrin Signaling	77	0.93	99%	0.47	90%	0.10	66%	0.01	51%	0.04	61%
B Cell Receptor Signaling	56	0.96	100%	0.65	96%	0.22	70%	0.00	50%	0.03	59%
Toll-like Receptor Signaling	25	0.97	100%	0.79	100%	0.06	68%	0.02	56%	0.28	80%
Production of Nitric Oxide and Reactive Oxygen Species in Macrophages	62	0.93	100%	0.60	92%	0.18	63%	-0.02	45%	0.06	61%
Role of Pattern Recognition Receptors in Recognition of Bacteria and Viruses	34	0.93	100%	0.22	82%	0.04	65%	0.01	50%	-0.02	50%
TREM1 Signaling	26	0.88	96%	0.33	92%	0.06	69%	-0.03	35%	0.02	54%
GM-CSF Signaling	30	0.94	100%	0.76	97%	0.25	70%	0.02	60%	0.00	43%
IL-6 Signaling	35	0.95	100%	0.68	100%	0.39	74%	0.22	71%	0.30	71%
IL-15 Signaling	33	0.96	100%	0.74	97%	0.11	58%	0.00	45%	0.04	58%
IL-8 Signaling	61	0.94	100%	0.48	87%	0.21	67%	-0.01	41%	0.03	51%
IL-1 Signaling	34	0.92	97%	0.74	100%	0.10	65%	0.03	59%	0.29	71%
IL-3 Signaling	34	0.95	100%	0.76	97%	0.12	56%	-0.02	44%	0.00	56%
PI3K/AKT Signaling	42	0.94	100%	0.36	86%	0.27	62%	0.05	60%	0.04	69%
p38 MAPK Signaling	37	0.94	100%	0.70	97%	0.34	73%	0.20	70%	0.29	65%
PPARα/RXRα Activation	55	0.94	98%	0.55	95%	0.16	53%	0.06	60%	0.19	64%
Leukocyte Extravasation Signaling	65	0.93	97%	0.67	95%	0.16	60%	-0.01	40%	0.29	71%
JAK/Stat Signaling	31	0.95	100%	0.73	97%	0.09	48%	0.00	52%	0.02	52%
Role of PKR in Interferon Induction and Antiviral Response	19	0.95	100%	0.71	95%	0.24	68%	0.10	63%	0.00	53%
Summary											
median		0.94	100%	0.67	95%	0.16	65%	0.01	51%	0.04	61%
minimum		0.88	96%	0.22	82%	0.04	48%	-0.04	35%	-0.02	43%
maximum		0.97	100%	0.79	100%	0.49	79%	0.22	71%	0.43	80%

Table S2B	# Genes	Human Trauma (R^2)	Human Trauma (%)	Human Endotoxemia (R^2)	Human Endotoxemia (%)	Mouse Burn (R^2)	Mouse Burn (%)	Mouse Trauma (R^2)	Mouse Trauma (%)	Mouse Endotoxemia (R^2)	Mouse Endotoxemia (%)
iCOS-iCOSL Signaling in T Helper Cells	53	0.94	100%	0.72	96%	0.20	68%	0.00	49%	-0.02	49%
CD28 Signaling in T Helper Cells	57	0.94	100%	0.69	98%	0.18	68%	0.04	61%	-0.02	47%
Calcium-induced T Lymphocyte Apoptosis	30	0.95	100%	0.77	100%	0.26	70%	0.03	63%	-0.11	40%
PKCθ Signaling in T Lymphocytes	53	0.94	100%	0.68	96%	0.26	75%	0.05	60%	0.00	51%
T Cell Receptor Signaling	47	0.96	100%	0.74	98%	0.32	68%	0.00	51%	-0.03	47%
Role of NFAT in Regulation of the Immune Response	72	0.94	100%	0.74	100%	0.22	74%	0.04	60%	0.00	49%
Primary Immunodeficiency Signaling	20	0.95	100%	0.38	80%	0.11	55%	0.01	60%	-0.02	35%
B Cell Development	12	0.90	100%	0.48	83%	0.14	67%	0.20	75%	0.01	42%
CTLA4 Signaling in Cytotoxic T Lymphocytes	46	0.92	100%	0.67	85%	0.18	70%	0.04	54%	0.00	48%
Antigen Presentation Pathway	18	0.75	89%	0.59	89%	0.11	67%	0.36	67%	-0.04	50%
EIF2 Signaling	67	0.92	97%	0.67	96%	0.05	61%	0.04	66%	0.00	52%
IL-4 Signaling	35	0.91	97%	0.61	91%	0.15	60%	0.03	54%	0.00	54%
NF-κB Activation by Viruses	30	0.96	100%	0.62	100%	0.16	63%	-0.01	47%	0.00	57%
Type I Diabetes Mellitus Signaling	48	0.93	100%	0.74	98%	0.24	67%	0.07	69%	0.00	46%
Cytotoxic T Lymphocyte-mediated Apoptosis of Target Cells	27	0.88	100%	0.79	96%	0.40	70%	0.07	67%	-0.29	30%
T Helper Cell Differentiation	32	0.94	100%	0.80	100%	0.03	53%	0.03	66%	-0.03	38%
Purine Metabolism	73	0.93	100%	0.38	85%	0.03	56%	0.12	66%	-0.08	33%
Regulation of eIF4 and p70S6K Signaling	52	0.94	96%	0.59	92%	0.12	58%	0.00	60%	0.04	60%
mTOR Signaling	61	0.92	97%	0.39	84%	0.07	59%	0.00	57%	-0.02	52%
OX40 Signaling Pathway	26	0.89	100%	0.75	100%	0.42	73%	0.30	77%	-0.05	35%
Summary											
median		0.93	100%	0.68	96%	0.17	67%	0.04	61%	-0.02	48%
minimum		0.75	89%	0.38	80%	0.03	53%	-0.01	47%	-0.29	30%
maximum		0.96	100%	0.80	100%	0.42	75%	0.36	77%	0.04	60%

Acknowledgements

List of additional participants and affiliations of the Inflammation and Host Response to Injury Large Scale Collaborative Research Program:

Amer Abouhamze, Dept. of Surgery, University of Florida College of Medicine, Gainesville, FL 32610.

Ulysses G.J. Balis, Dept. of Pathology, University of Michigan Medical School, Ann Arbor, MI 48109

David G. Camp II, Pacific Northwest National Laboratory, Richland, WA 99352

Asit K. De, Dept. of Surgery, University of Rochester Medical Center, Rochester, NY 14642

Brian G. Harbrecht, Dept. of Surgery, University of Louisville, Louisville, KY 40292

Douglas L. Hayden, Biostatistics Center, Massachusetts General Hospital, Boston, MA 02114

Amit Kaushal, Stanford Genome Technology Center, Stanford University, Palo Alto, CA 94305

Grant E. O'Keefe, Dept. of Surgery, University of Washington, Seattle, WA 98104

Kenneth T. Kotz, Dept. of Surgery, Massachusetts General Hospital, Boston, MA 02114

Weijun Qian, Pacific Northwest National Laboratory, Richland, WA 99352

David A. Schoenfeld, Biostatistics Center, Massachusetts General Hospital, Boston, MA 02114

Michael B. Shapiro, Dept. of Surgery, Northwestern University, Chicago, IL 60611

Geoffrey M. Silver, Dept. of Surgery, Loyola University School of Medicine, Maywood, IL 60153

Richard D. Smith, Pacific Northwest National Laboratory, Richland, WA 99352

John D. Storey, Dept. of Molecular Biology, Princeton University, Princeton, NJ 08544

Robert Tibshirani, Dept. of Statistics, Stanford University, Stanford, CA 94305

Mehmet Toner, Dept. of Surgery, Massachusetts General Hospital, Boston, MA 02114

Julie Wilhelmy, Stanford Genome Technology Center, Stanford University, Palo Alto, CA 94305

Bram Wispelwey, Biostatistics Center, Massachusetts General Hospital, Boston, MA 02114

Wing H Wong, Dept. of Statistics, Stanford University, Stanford, CA 94305

Supplemental References:

1. Storey JD, *et al.* (2005) Significance analysis of time course microarray experiments. *Proc Natl Acad Sci U S A.,* 102(36):12837-42.
2. Blake JA, *et al.* (2011) The Mouse Genome Database (MGD): premier model organism resource for mammalian genomics and genetics. *Nucleic Acids Res.,* 39(Database issue):D842-8.
3. Dressman HK, *et al.* (2007) Gene expression signatures that predict radiation exposure in mice and humans. *PLoS Med.,* 4(4):e106.
4. Meadows SK, *et al.* (2008) Gene expression signatures of radiation response are specific, durable and accurate in mice and humans. *PLoS One,* 3(5):e1912.